

On the Collision Nature of Two Coronal Mass Ejections: A Review

Fang Shen^{1,2,3} · Yuming Wang⁴ · Chenglong Shen⁴ ·
Xueshang Feng^{1,2,3}

Received: 19 September 2016 / Accepted: 19 June 2017 / Published online: 2 August 2017
© The Author(s) 2017. This article is published with open access at Springerlink.com

Abstract Observational and numerical studies have shown that the kinematic characteristics of two or more coronal mass ejections (CMEs) may change significantly after a CME collision. The collision of CMEs can have a different nature, *i.e.* inelastic, elastic, and superelastic processes, depending on their initial kinematic characteristics. In this article, we first review the existing definitions of collision types including Newton's classical definition, the energy definition, Poisson's definition, and Stronge's definition, of which the first two were used in the studies of CME–CME collisions. Then, we review the recent research progresses on the nature of CME–CME collisions with the focus on which CME kinematic properties affect the collision nature. It is shown that observational analysis and numerical simulations can both yield an inelastic, perfectly inelastic, merging-like collision, or a high possibility of a superelastic collision. Meanwhile, previous studies based on a 3D collision picture suggested that a low approaching speed of two CMEs is favorable for a superelastic nature. Since CMEs are an expanding magnetized plasma structure, the CME collision process is quite complex, and we discuss this complexity. Moreover, the models used in both

Earth-affecting Solar Transients

Guest Editors: Jie Zhang, Xochitl Blanco-Cano, Nariaki Nitta, and Nandita Srivastava

✉ F. Shen
fshen@spaceweather.ac.cn

Y. Wang
ymwang@ustc.edu.cn

C. Shen
clshen@ustc.edu.cn

X. Feng
fengx@spaceweather.ac.cn

¹ SIGMA Weather Group, State Key Laboratory of Space Weather, National Space Science Center, Chinese Academy of Sciences, Beijing 100190, China

² HIT Institute of Space Science and Applied Technology, Shenzhen 518055, China

³ University of Chinese Academy of Sciences, Beijing 100049, China

⁴ School of Earth and Space Sciences, University of Science and Technology of China, Hefei 230026, China

observational and numerical studies contain many limitations. All of the previous studies on collisions have not shown the separation of two colliding CMEs after a collision. Therefore the collision between CMEs cannot be considered as an ideal process in the context of a classical Newtonian definition. In addition, many factors are not considered in either observational analysis or numerical studies, *e.g.* CME-driven shocks and magnetic reconnections. Owing to the complexity of the CME collision process, a more detailed and in-depth observational analysis and simulation work are needed to fully understand the CME collision process.

Keywords Coronal mass ejections · Collision nature · Interaction

1. Introduction

Coronal mass ejections (CMEs) have been observed remotely since the early 1970s with the *Orbiting Solar Observatory 7* (OSO-7: Tousey *et al.*, 1973) and *Skylab* (MacQueen *et al.*, 1974). In one of the early studies, Burlaga, Behannon, and Klein (1987) reported the interaction of successive interplanetary CMEs (ICMEs) between the Sun and the Earth observed during the 1980s using multispacecraft *in situ* measurements from the twin *Helios* satellites. Later, it was shown from coronagraphic observations and solar wind measurements at 1 AU that some successive ICMEs can merge with each other and form a compound structure (*e.g.* Burlaga, Plunkett, and St. Cyr, 2002; Lugaz and Roussev, 2011). Alternatively, when two or more magnetic clouds (MCs) interact, that is, a subset of CME ejecta that contains well-organized helical magnetic field lines, they may form multiple-MC structures and display distinct solar wind signatures and a geoeffectiveness that is different from isolated MCs or compound structures (Wang, Wang, and Ye, 2002; Wang, Ye, and Wang, 2003). CME interactions and the resulting complex structures have been widely reported and studied in observations and magnetohydrodynamics (MHD) simulations (*e.g.* Gopalswamy *et al.*, 2001; Schmidt and Cargill, 2004; Lugaz, Manchester, and Gombosi, 2005; Burlaga, Plunkett, and St. Cyr, 2002; Wang, Ye, and Wang, 2003; Farrugia and Berdichevsky, 2004; Wu, Wang, and Gopalswamy, 2002; Hayashi, Zhao, and Liu, 2006; Xiong *et al.*, 2007).

Thanks to the wide field of view (FOV) of the *Sun Earth Connection Coronal and Heliospheric Investigation/Heliospheric Imagers* (SECCHI/HI: Howard and Tappin, 2008) onboard the *Solar Terrestrial Relations Observatory* (STEREO: Kaiser *et al.*, 2008), a mission successfully launched in 2006, interactions of CMEs in interplanetary space have been more frequently observed. This largely stimulated the observational and numerical studies in this area (*e.g.* Gopalswamy *et al.*, 2009; Xiong, Zheng, and Wang, 2009; Lugaz *et al.*, 2009, 2012, 2013, Lugaz, Vourlidas, and Roussev, 2009; Temmer *et al.*, 2012, 2014; Shen *et al.*, 2012a; Liu *et al.*, 2012, 2014; Martínez-Oliveros *et al.*, 2012; Webb *et al.*, 2013; Shen *et al.*, 2011, 2012b, 2013, 2016; Mishra and Srivastava, 2014; Mishra, Srivastava, and Chakrabarty, 2015; Mishra, Srivastava, and Singh, 2015; Mishra, Wang, and Srivastava, 2016; Shanmugaraju *et al.*, 2014; Colaninno and Vourlidas, 2015). A comprehensive review about the interaction of successive CMEs and consequences in particle acceleration and geoeffectiveness by Lugaz *et al.* (2017) can be found in the Topical Collection called Earth-affecting Solar Transients.

Before discussing the main topic of this review, we wish to clarify two terms: “interaction” and “collision”, which have frequently appeared in the literature in relation to the

interaction of successive CMEs. A CME contains a core that is a magnetized plasma structure, a compressed solar wind shell, and a driven shock if it propagates fast enough. Generally speaking, a process that involves magnetic flux and momentum and energy exchange in multiple CMEs can be referred to as “CME–CME interaction”. In this process, if the main bodies of the two CMEs touch at some stage, we refer to the process as a “CME–CME collision”. This means that collisions are a subset of interactions. This is consistent with the usage of the two terms in Mishra and Srivastava (2014). The main body here refers to the CME core, *i.e.* the magnetized plasma structure and the ambient compressed solar wind shell, as it is impossible to distinguish between the two parts in current imaging data. A collision process may significantly change the kinematics of colliding CMEs, *e.g.* their speeds and propagation directions, and hence influence the effects they have on space weather. The current knowledge about the nature of the CME collision, which we discuss in Section 2, may be used to predict their post-collision kinematics and hence their arrival time (Mishra, Wang, and Srivastava, 2016).

The first observational case of a CME–CME interaction and/or collision was reported by Gopalswamy *et al.* (2001). In this case, two colliding CMEs were assumed to merge. A merging process can be treated as a special inelastic collision, sometimes referred to as superinelastic behavior (*e.g.* Schmidt and Cargill, 2004; Temmer *et al.*, 2012). The first discussion of the momentum exchange during a CME–CME interaction appeared in Lugaz, Vourlidas, and Roussev (2009), who proposed four interaction scenarios. The first detailed and comprehensive study focusing on the collision nature between two CMEs was presented by Shen *et al.* (2012a), who proposed a superelastic behavior in the collision of CMEs. This promoted a series of subsequent studies. While some studies have shown the possibility of a superelastic collision of CMEs (*e.g.* Shen *et al.*, 2012a, 2013; Colaninno and Vourlidas, 2015), (perfectly) inelastic collisions (*e.g.* Lugaz *et al.*, 2012; Maričić *et al.*, 2014; Mishra, Srivastava, and Chakrabarty, 2015) and nearly elastic collisions (Mishra and Srivastava, 2014; Mishra, Srivastava, and Singh, 2015) were also reported. This raises the question as to what controls the nature of the CME collision.

In this review, starting from the definitions of collision types (Section 2), we summarize previous studies and the current knowledge on the nature of the collision of CMEs (Section 3), focusing on the numerical methods developed for simulating CME–CME collisions (Section 4). A summary and discussion are given in Section 5.

2. Definition and Determination of the Collision Types

From Newton’s experimental law of collision, the coefficient of restitution, e , is defined as the ratio of relative speeds after and before the collision (defined as approaching speed and separating speed, respectively) (Saitoh *et al.*, 2010). If we denote the velocities of the preceding CME (CME1) and the following CME (CME2) before the collision in an inertial frame by u_1 and u_2 along the line of the collision, and the corresponding velocities after the collision by v_1 and v_2 , the coefficient of restitution is written as

$$e = -\frac{v_1 - v_2}{u_1 - u_2}. \quad (1)$$

Based on the value of e , collisions are classified into different types. Normally, the value of e is between 0 and 1. The collision is perfectly inelastic when $e = 0$. When $0 < e < 1$, the collision belongs to the inelastic type, and when $e = 1$, it is an elastic collision. However, as mentioned by Shen *et al.* (2012a), abnormal values of e , such as $e > 1$ or $e < 0$, have been

reported (Louge and Adams, 2002; Saitoh *et al.*, 2010). Especially when $e > 1$, the collision is superelastic (Saitoh *et al.*, 2010).

The change in kinetic energy (or mechanical energy if the gravitational potential energy of the colliding system changes) is also often used to classify the collision type. For example, a decrease in kinetic energy implies an inelastic collision, no change in kinetic energy implies an elastic collision, and an increase in kinetic energy implies a superelastic collision. In this way (hereafter called “energy definition”), the collision nature depends on whether the kinetic energy of the colliding system is converted into other forms of energy or is reversed, *i.e.* the direction of the energy conversion during a collision. Generally, a rather simple picture of collision is considered: the colliding objects cannot expand or contract. In this case, the above energy definition is equivalent to the classical Newtonian definition based on König’s theorem (König, 1905), which points out that the total kinetic energy of a group of particles in an inertial coordinate system is equal to the kinetic energy of the centroid of the particles in the inertial system plus the sum of the kinetic energy for every particle in the centroid coordinate system. For two colliding objects with mass of m_1 and m_2 , it can be deduced from the theorem (König, 1905) that before a collision

$$T_0 = T_{0c} + \frac{1}{2} \frac{m_1 m_2}{m_1 + m_2} (u_1 - u_2)^2, \quad (2)$$

and after the collision

$$T = T_c + \frac{1}{2} \frac{m_1 m_2}{m_1 + m_2} (v_2 - v_1)^2, \quad (3)$$

where T_0 and T are the total kinetic energy of the two colliding objects, and T_{0c} and T_c are the total centroid kinetic energy of the two colliding objects in an inertial coordinate system before and after the collision, respectively. Considering the momentum conservation law, we have $T_{0c} = T_c$. Therefore, it could be easily deduced from Equations 1–3 that the relationship between e and unity is equivalent to the relationship between T and T_0 . However, the two definitions are usually not equivalent for two expanding objects unless their expansion speeds do not change during the collision.

In addition to the classical Newtonian definition and the energy definition, there are two other definitions of the coefficient of restitution suggested by Poisson and by Stronge, respectively (Brach, 1984; Brogliato, 1996; Stewart, 2000; Lubarda, 2010). In Poisson’s kinetic definition (hereafter called “Poisson’s definition”), the coefficient of restitution, e_p , is defined as the ratio of the magnitudes of the normal impulses corresponding to the periods of restitution and compression. In the cases of frictionless collisions, the expression of e_p is proved to be the same as that from the classical Newtonian definition (*e.g.* Beer, Johnston, and Clausen, 2007). However, in the presence of friction, the two definitions are not equivalent (Keller, 1986; Brogliato, 1996; Lubarda, 2010). Thus, in practice, the classical Newtonian definition and Poisson’s definition of the coefficient of restitution are consistent with each other (Wang and Mason, 1992).

Stronge (1990) introduced an energetic coefficient of restitution (hereafter called “Stronge’s definition”), e_s , whose square is equal to the negative ratio of the elastic strain energy released during the restitution phase, W_r , and the internal energy of deformation absorbed during the compression phase of the collision, W_c , *i.e.* $e_s^2 = -\frac{W_r}{W_c}$ (also see Brogliato, 1996; Lubarda, 2010; Yao, Chen, and Liu, 2005). In the case of an eccentric collision, in which the normal line perpendicular to the contact surface of the two bodies in collision is different from the line between the centroids of the two bodies, or velocities slip reversal, which means that the velocities change to

the opposite directions, the value of e_s depends on the initial orientation of the bodies in collision, the friction, the internal sources of dissipation, *etc.* (Brogliato, 1996; Lubarda, 2010).

Lubarda (2010) demonstrated that the energetic coefficient of restitution defined by Stronge was a geometric mean of the coefficients of restitution defined by Newton and Poisson. In the case of an eccentric collision with the presence of friction, Stronge's definition is shown to be the only one that is energetically consistent, whereas both Newton's and Poisson's definitions result in an energy loss. The classical definitions of Newton, Poisson, and Stronge are equivalent if a slip neither reverses nor stops (Lubarda, 2010).

Summarizing, there are various ways to define the coefficient of restitution. All of the previous studies on the nature of CME–CME collisions used the classical Newtonian definition or energy definition. However, CMEs are not solid objects, they may expand or contract with a changing speed. Thus, the energy definition may not be equivalent to the classical Newtonian definition unless the change of the expansion or contraction speed is ignored. We suggest that the energy definition is more general than the classical Newtonian definition because it defines the direction of the energy conversion during a collision, which is a better way to estimate the nature of the collision for objects that may expand or contract with different speeds after the collision.

3. Estimating the Nature of the CME Collision from Observations

3.1. CME Kinematics

To study the nature of the CME collision, we need to calculate the true masses (Colaninno and Vourlidas, 2009) and the speeds of two colliding CMEs. The most widely used method to determine the mass of a CME is based on the Thomson scattering theory (Jackson, 1997). This theory enables us to use the observed brightness of a coronal structure to estimate the density of electrons under certain assumptions (*e.g.* Vourlidas and Howard, 2006, and the references therein). By assuming that the mass of the observed CME is located in the plane of the sky, the CME mass can be calculated from calibrated coronagraph images from the *Solar and Heliospheric Observatory* (SOHO) (*e.g.* Vourlidas *et al.*, 2000). In the STEREO era, Colaninno and Vourlidas (2009) then improved the method by assuming that the same masses should be derived based on the coronagraph images from STEREO-A and -B. They used this assumption as a constraint to simultaneously derive the propagation direction and the total true mass of a CME. It was noted by Colaninno and Vourlidas (2009) that their method has an error of $\sim 15\%$.

The graduated cylindrical shell (GCS) model developed by Thernisien, Howard, and Vourlidas (2006, see also Thernisien, Vourlidas, and Howard, 2009 and Thernisien, 2011) has been frequently used to fit the geometry of a CME in coronagraph observations, which is assumed to be a flux-rope-like structure. The derived parameters from the GCS model include the angular width, velocity, and propagation direction of a CME. The propagation direction can also be used as an additional constraint in the mass estimate, as demonstrated in Feng, Inhester, and Gan (2015), Feng *et al.* (2015).

The tie-pointing method, a kind of triangulation technique (Thompson, 2009), is an efficient method to derive the true kinematics of CMEs by tracking and triangulating selected features along the leading edge of the CMEs (Mishra, Srivastava, and Chakrabarty, 2015). It uses the concept of epipolar geometry (Inhester, 2006), and the same features in images from

STEREO-A and -B are identified along the same epipolar line in both images. A similar triangulation method is used to track CMEs in the heliosphere, based on time-elongation maps constructed from SECCHI/HI (Liu *et al.*, 2010). Taking advantage of stereoscopic imaging observations from STEREO-A and -B, these methods can determine the propagation direction and radial distance of CMEs.

To obtain the kinematic parameters of CMEs as they propagate in the interplanetary space, the point-P and fixed- φ (FP) methods are often used (Kahler and Webb, 2007; Howard *et al.*, 2007; Wood *et al.*, 2009). The point-P method assumes that the ICME front is always tangent to the solar limb, which provides the lower limit of the distance of the CME front. The FP method assumes that the CME is a relatively compact structure moving radially from the Sun. By assuming a CME is an expanding self-similar sphere, Lugaz, Vourlidas, and Roussev (2009) derived an analytical relationship between elongation angle and radial distance of a propagating CME. This relationship is the harmonic mean (HM) of the point-P and FP approximations. The tangent-to-a-sphere method (Lugaz *et al.*, 2010), which is based on the HM geometry, is also used in the case of CME–CME interaction to track the true kinematics of CMEs.

As the separation angle of the STEREO spacecraft increases, the 3D reconstruction of CMEs could be cross-checked by two independent methods. Mishra, Srivastava, and Chakrabarty (2015) used a tie-pointing procedure on SCEECHI/COR2 data to estimate the true kinematics of two CMEs. Then, they also visually fit the two CMEs in the SECCHI/COR2 FOV using the GCS model. Their results showed that a combination of the tie-pointing method and the GCS forward-modeling is more accurate than a single model to estimate the kinematics of CMEs in the FOV of coronagraphs.

3.2. The Nature of the CME Collision

While the actual collision of CMEs can be considered as a 3D process, it is most often explicitly or implicitly approximated as a 1D process because of the limitation of the observational technique and inversion method. According to the different methods for estimating the nature of the CME collision, the progress achieved has been based mainly on three approaches, treating the collision of CMEs as i) a simple 1D head-on collision, ii) a 1D head-on collision with momentum-conservation constraint, and iii) an oblique collision in 3D.

3.2.1. 1D Head-on Collision

Lugaz, Vourlidas, and Roussev (2009) analyzed two CMEs during 24–27 January 2007. They used different methods (point-P, FP, and HM) to derive the position of CME features from elongation-angle measurements made by SECCHI or the *Solar Mass Ejection Imager* (SMEI; Webb *et al.*, 2009). Before collision, these methods gave an average speed of $\sim 600 \text{ km s}^{-1}$ at $\sim 40 R_{\odot}$ for the first CME front. For the second CME front, a speed of approximately $1200\text{--}1300 \text{ km s}^{-1}$ was found at $\sim 20 R_{\odot}$. After the collision, the average speed of the first front was about $850\text{--}900 \text{ km s}^{-1}$. The second front had a speed of $750\text{--}850 \text{ km s}^{-1}$ at $\sim 100 R_{\odot}$ and later decelerated to $500\text{--}600 \text{ km s}^{-1}$. Therefore, it was found that the preceding front was faster than the following front after the collision. Four scenarios were given to explain the phenomenon, three of which fall into the category of a 1D head-on CME–CME collision, as shown in Figure 1.

Using HI observations from STEREO and *in situ* observations, Liu *et al.* (2012, 2014) studied the Sun-to-Earth characteristics of the CME–CME interaction process observed during 30 July–1 August 2010 (Liu *et al.*, 2012) and during 25–27 September 2012 (Liu *et al.*,


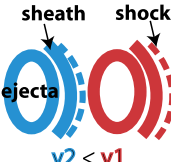








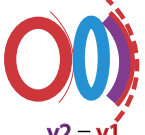

Before Collision	Intermediate Step(s)			After Collision
<p>No interaction</p>  <p>$v_2 > v_1$</p>				<p>sheath shock</p>  <p>$v_2 < v_1$</p>
<p>Perfectly inelastic</p>  <p>$v_2 > v_1$</p>	<p>Remark: For scenarios 2 and 3, the red shock may or may not dissipate during the collision.</p>			 <p>$v_2 = v_1$</p>
<p>Mysterious collision</p>  <p>$v_2 > v_1$</p>	<p>Momentum transfer between red and blue lasts ~ 12 hours to 1 day.</p>  <p>$v_2 = v_1$</p>			 <p>$v_2 < v_1$</p>
<p>Shock propagation</p>  <p>$v_2 > v_1$</p>	<p>v_2 corresponds to the <i>pile-up mass</i>, decelerating.</p>  <p>$v_2 > v_1$</p>	<p>v_2 corresponds to the <i>twice-compressed sheath</i>.</p>  <p>$v_2 > v_1$</p>	<p>v_1 corresponds to the <i>new sheath</i>.</p>  <p>$v_2 = v_1$</p>	<p>v_2 decreases because <i>this part of the sheath</i> is not driven.</p>  <p>$v_2 < v_1$</p>

Figure 1 Four possible scenarios for CME–CME head-on collisions. The *ellipses, solid arcs, and dashed arcs* correspond to the ejecta, dense sheaths, and to the shock waves, respectively (from Lugaz, Vourlidis, and Roussev, 2009). This figure is licensed under a Creative Commons Attribution 3.0 License.

2014). Their results indicate that the two collisions were inelastic based on the 1D head-on collision assumption, even though the propagation directions of the two colliding CMEs in each event were different.

The interaction of two CMEs during the 1 August 2010 events was also studied by Temmer *et al.* (2012) using STEREO/SECCHI COR and HI data. Before the collision, the geometric triangulation technique (Liu *et al.*, 2010) was applied to derive the propagation direction and radial distance of the two CMEs. Moreover, they also used FP and HM methods to find constant propagation directions and speeds. The masses of the two CMEs were calculated by stereoscopic image pairs from COR1 and COR2. Their results suggested that at the time of interaction, *i.e.* about 10 UT, the speeds of the first and the second CMEs were about 600 and 1400 km s⁻¹, respectively, and the mass of the second CME was about three times higher than that of the first CME. If the collision between the two CMEs were perfectly inelastic, the second CME was expected to move with a speed of ~ 1200 km s⁻¹, and if it were elastic, the first CME would accelerate to ~ 1800 km s⁻¹. However, from observations, the speed for the leading edge of the merged structure was derived to be ~ 800 km s⁻¹ at about 15 UT, which was even slower than the perfectly inelastic collision scenario.

Combining *in situ* measurements and heliospheric imaging, Lugaz *et al.* (2012) studied two interacting CMEs during 23–24 May 2010. In order to derive the directions of the CMEs observed by COR2 and H11 FOVs, they applied the GCS model, the tangent-to-a-sphere, and the HM methods. The CME kinematics up to 0.4 AU, including the evolution of the CME expansion, was derived. They found that during the interaction, the speed of the following CME decelerated from close to 600 km s^{-1} to 380 km s^{-1} , and the preceding CME was only slightly accelerated from $\sim 300 \text{ km s}^{-1}$ to 380 km s^{-1} . They pointed out that the changes in the speeds of the two CMEs were consistent with a perfectly inelastic collision.

Another set of widely studied successive ICMEs occurred during 13–15 February 2011, which consisted of three Earth-directed CMEs (*e.g.* Temmer *et al.*, 2014; Maričić *et al.*, 2014; Shanmugaraju *et al.*, 2014; Mishra and Srivastava, 2014). Temmer *et al.* (2014) presented a detailed study of the interaction process of two CMEs launched on 14 February and 15 February. During the interaction, the 14 February CME accelerated from ~ 400 to $\sim 700 \text{ km s}^{-1}$ and that of 15 February CME decelerated from ~ 1300 to $\sim 600 \text{ km s}^{-1}$. They found that a simplified scenario such as an inelastic collision may not be sufficient to describe the loss of the total kinetic energy of the CMEs during the CME–CME interaction. Maričić *et al.* (2014) studied the heliospheric propagation and some space weather aspects of these three CMEs. They determined that there was an obvious increase in the 14 February CME speed from 400 to 600 km s^{-1} , during which it moved from ~ 28 to $\sim 45 R_{\odot}$, whereas the speed of the 15 February CME decelerated to 600 km s^{-1} from its maximum speed of 1300 km s^{-1} . Their results showed that after the momentum transfer was completed, the two CMEs continued to move together at the same speed, as expected in inelastic collisions.

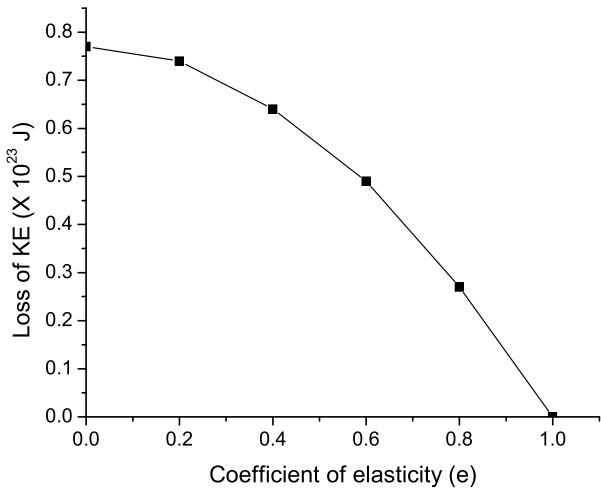
The analysis by Shanmugaraju *et al.* (2014) on the set of CMEs focused on the change in kinetic energy of the CMEs during the interaction between the 14 February CME and 15 February CME. Under the assumption of a head-on collision, *i.e.* the same propagation direction of the two CMEs, they deduced that the loss of kinetic energy in terms of initial velocities could be written as

$$\Delta E = m_1 m_2 [1 - e^2] [u_1 - u_2]^2 / [2(m_1 + m_2)]. \quad (4)$$

From the equation, they obtained the loss of kinetic energy, ΔE , as a function of the coefficient of restitution (“ e ”), as shown in Figure 2. For a perfectly inelastic collision, *i.e.* $e = 0$, the loss of kinetic energy attained maximum value, which was estimated to be $0.77 \times 10^{23} \text{ J}$ using the speeds derived from the *Large Angle and Spectroscopic Coronagraph* (LASCO) data. For this event, their analysis suggested an inelastic collision.

We note that all the results described in this section indicate that the type of collision is inelastic, perfectly inelastic, or a merging-like process (superinelastic collision). The reason might have been the biased assumption of a head-on collision. We also remark that most of the speeds used to estimate the nature of the collision of CMEs in the aforementioned studies are the speeds of their leading edges, which include the propagation speed and expansion speed. CMEs usually propagate at a constant angular width (Schwenn *et al.*, 2005), *i.e.* experience an approximately self-similar expansion. Thus, the ratio of expansion speed to propagation speed of a CME is approximately proportional to the sine of the half-angular width of the CME. According to the analysis of limb CMEs by Wang *et al.* (2011), the average value of the angular widths of CMEs is about 59° , suggesting that the value of the expansion speed is half of the propagation speed or one-third of the speed of the leading edge, which is significant. Thus, the propagation speed rather than the leading-edge speed should be used when studying the nature of the collision of CMEs in the context of the classical Newtonian definition, although the leading-edge speed is relatively easy to derive

Figure 2 Loss of kinetic energy versus coefficients of elasticity or restitution plotted for CME speeds measured using LASCO data (from Shanmugaraju *et al.*, 2014).



from imaging data and may be appropriate to determine the final speeds of the colliding CMEs, which is the main objective of the above mentioned studies. However, to use the propagation speed from remote observations in determining the collision nature, the changes in the expansion speeds of the two CMEs must be determined. One way to better constrain the derived speeds in order to determine the nature of the collision of CMEs is to add a constraint of conservation of momentum, but still treating the collision as a 1D head-on collision.

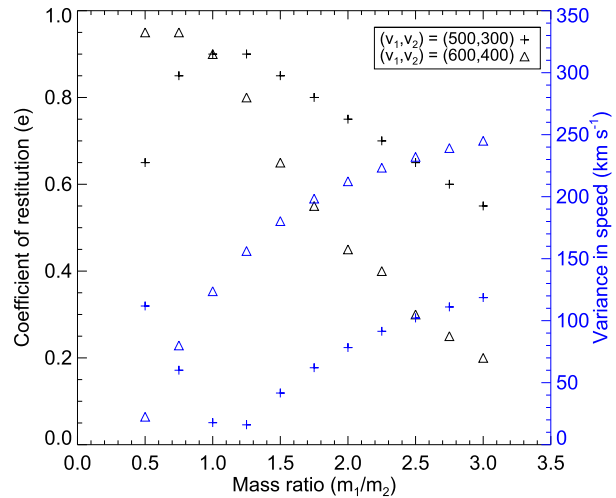
3.2.2. 1D Head-on Collision with Momentum Conservation Constraint

For a collision, an important issue is to know if the momentum conservation is satisfied, which was not considered in the aforementioned studies, although the simplest head-on collision model was assumed. The first attempt to satisfy the momentum conservation law was made by Mishra and Srivastava (2014), who also studied the three interacting CMEs during 13–15 February 2011. They applied the stereoscopic methods, including the stereoscopic self-similar expansion (SSSE) method by Davies *et al.* (2013), the GCS model by Thernisien, Vourlidas, and Howard (2009), and the tangent-to-a -sphere method by Lugaz *et al.* (2010), to yield the kinematics of these CMEs. They estimated the true masses of the CMEs by using the simultaneous image pair of SECCHI/COR2 (Colaninno and Vourlidas, 2009) based on the Thomson scattering theory. With these parameters, they analyzed the nature of the collision between the 14 and 15 February CMEs under the assumption of a 1D head-on collision. In their analysis, the momentum conservation was considered and used to constrain the velocities of the CMEs. If the velocities before and after the collision derived from the observations are used, the conservation of momentum may not be satisfied. Therefore, Mishra and Srivastava (2014) calculated the expected theoretical velocities, v_{th} , of the 14 and 15 February CMEs after the collision so that the conservation of momentum was satisfied for a given value of e as follows:

$$v_{1th} = \frac{m_1 u_1 + m_2 u_2 + m_2 e(u_2 - u_1)}{m_1 + m_2} \quad \text{and} \quad (5)$$

$$v_{2th} = \frac{m_1 u_1 + m_2 u_2 + m_1 e(u_1 - u_2)}{m_1 + m_2}.$$

Figure 3 Best-suited restitution coefficients corresponding to different mass ratios for the 14 and 15 February CMEs are shown for their observed velocities in the post-collision phase (in *black*). The variance in speed corresponding to the estimated best-suited restitution coefficient is also shown in *blue* (from Mishra and Srivastava, 2014). The figure is reproduced by permission of the American Astronomical Society (AAS).



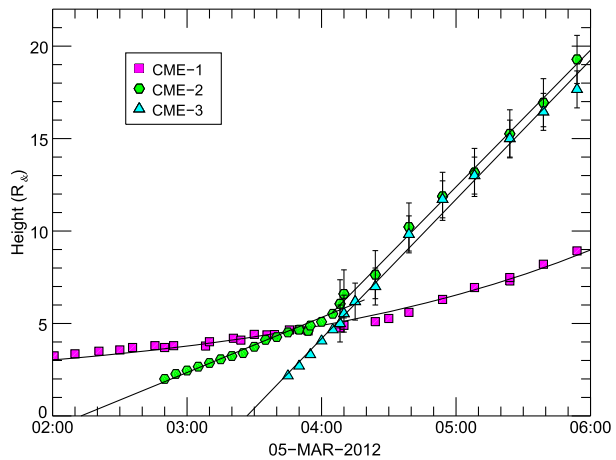
The subscript *th* in these equations means that the velocities were theoretically estimated. Using the true mass values and the velocities of the 14 and 15 February CMEs before collision, they obtained a set of expected velocities, v_{1th} and v_{2th} , after the collision. Furthermore, the authors compared these expected values with the derived values from the observations by calculating the variance σ as

$$\sigma = \sqrt{(v_{1th} - v_1)^2 + (v_{2th} - v_2)^2}. \tag{6}$$

The best value of e was then determined by minimizing the variance. Figure 3 shows the minimum variance as well as the corresponding value of e for different ratios of the CME masses. The figure also shows that the nature of the collision remained in the inelastic regime and was unable to reach a perfectly inelastic ($e = 0$), elastic ($e = 1$), or superelastic ($e > 1$) regime for this event.

Mishra, Srivastava, and Chakrabarty (2015) later analyzed the collision and post-collision characteristics of two CMEs during 9–10 November 2012 using STEREO/SECCHI and *in situ* observations. To determine the directions and speeds of the CMEs more accurately and to track the CMEs in the HI FOV, the tie-pointing method (Thompson, 2009), the GCS forward modeling (Thernisien, Vourlidas, and Howard, 2009), the J-maps method (Davies *et al.*, 2009), and the HM method (Lugaz, Vourlidas, and Roussev, 2009) were applied to study the interacting CMEs. Similar to their previous study (Mishra and Srivastava, 2014), the true masses of the CMEs were estimated to understand the momentum exchange scenario during the collision. The authors varied the value of e within a reasonable range and estimated the corresponding expected velocities, v_{1th} and v_{2th} , of the post-collision CMEs by using Equations 5. Equation 6 was used to determine the optimal value of e . Their results showed that the nature of the observed collision remained almost perfectly inelastic. These calculations also supported the claim that a significant exchange of kinetic energy and momentum took place during the CME–CME collision (Temmer *et al.*, 2012; Lugaz *et al.*, 2012; Shen *et al.*, 2012a; Maričić *et al.*, 2014). In the same year, Mishra, Srivastava, and Singh (2015) used the same method to study the kinematics of the interacting CMEs of 25 and 28 September 2012. The collision of these two CMEs was found to be close to elastic. A large momentum exchange and kinetic energy change occurred during the interaction.

Figure 4 Height-time plot for CME-1 (magenta squares), CME-2 (green hexagons), and CME-3 (blue triangles) based on the GCS fits and the functions fitted to the data (black) (from Colaninno and Vourlidas, 2015). Reproduced by permission of the AAS.



Although the momentum conservation law was used to constrain the calculation, the model still assumes a 1D head-on collision. In fact, the propagation directions of the two colliding CMEs in each case were not the same in the studies by Mishra and Srivastava (2014), Mishra, Srivastava, and Chakrabarty (2015), and Mishra, Srivastava, and Singh (2015). The angle between the propagation directions of the two CMEs was about 20° , 15° , and 28° , respectively. On the other hand, the deflection of the CMEs that resulted from the collision was also reported (e.g. Lugaz *et al.*, 2012; Shen *et al.*, 2012a). Thus a 1D head-on collision is not the best approximation for these events. In addition, the speeds of the studied CMEs were for their leading edges instead of their propagation speeds, which results in large errors, as has been discussed at the end of the previous section.

3.2.3. Analysis of the Collisions in 3D

A relatively more precise analysis is that performed in 3D using the propagation speed. Using STEREO/SECCHI and *in situ* observations, Shen *et al.* (2012a) studied a CME collision event on 2–8 November 2008, which was for the first time suggested to be superelastic. The authors applied the GCS model and J-maps to analyze the dynamics of the CMEs and their collision. The masses of the CMEs were calculated from calibrated coronagraph images (Vourlidas *et al.*, 2000). The two interacting CMEs were treated as two elastic balls, and the approaching speed was defined as the speed of the centroid of one ball relative to the other along the collision direction. By considering the uncertainties in the propagation directions and the velocities of the two CMEs, Shen *et al.* (2012a) found that the collision was probably superelastic with a 73% probability, wherein the total kinetic energy of the collision system increased by about 6.6%. In this work, the collision between the CMEs was not considered as a head-on collision and the analysis was made in 3D space. The conservation of momentum was indirectly evaluated by analyzing the effect of the solar wind on the acceleration of the first CME, which was found to be negligible compared to that of the collision itself.

Using multiple-viewpoint observations from SOHO, STEREO-A, and STEREO-B, Colaninno and Vourlidas (2015) studied the interaction of three CMEs observed on 5 March 2012 denoted as CME-1, CME-2, and CME-3. The authors applied the GCS model to analyze the kinematics of the three CMEs as shown in Figure 4. There was a clear and visible interaction between CME-2 and CME-3; CME-2 quickly accelerated to the same velocity

as CME-3 and was deflected from its initial trajectory by about 24° ; while CME-3 maintained a constant velocity. These authors' results suggested that the kinetic energy of the system might have increased during the collision, indicating the possibility of a superelastic collision.

Recently, Mishra, Wang, and Srivastava (2016) have attempted to investigate how the characteristics of CMEs, *e.g.* propagation direction, propagation speed, expansion speed, angular size, and mass, influence the nature of the collision in 3D. The authors analyzed the interacting CMEs that were launched on 25 October 2013 using STEREO observations. Similar to their previous studies, the GCS model and the self-similar expansion (SSE) method (Davies *et al.*, 2012) were applied to estimate the CME kinematics. The propagation and expansion speeds, angular size, collision direction, and the masses of the CMEs, which were derived from imaging observations, were considered in the analysis. The results of this work revealed that a expansion speed of the following CME comparatively higher than that of the preceding CME tended to increase the probability of a superelastic collision, which is consistent with the results obtained by Shen *et al.* (2016). From the analysis of the interacting CMEs of 25 October 2013, the relative expansion speed of the CMEs seemed to be more important than the relative approaching speed for determining the nature of the collision. It should be mentioned that because of the large uncertainties in the parameters, including the velocity and propagation direction, in spite of considering the momentum conservation constraint and the oblique collision in 3D, there still exist some problems, *e.g.* the disagreement of the final velocities with the *in situ* measurements (Mishra, Srivastava, and Singh, 2015), which suggest that the ambient solar wind participated in the momentum exchange.

4. Simulating CME–CME Collisions Using Numerical Methods

Numerical simulations can be used to study CME–CME collision more realistically than the aforementioned analyses. Although a relatively large number of simulations of CME–CME interactions have been performed, only a few investigations of the nature of the collisions have been based on numerical simulations so far.

Schmidt and Cargill (2004) studied the oblique collision of two CMEs using a 2.5D MHD numerical simulation from 1.7 to $32 R_\odot$. In this model the density and the three components of the velocity and the magnetic field are all functions of time, the radial distance, and the meridional angle. Initially, the two CMEs had the same rotation of the magnetic field, and were separated by 40° in the meridional plane, and later the two CMEs were set with an opposite rotation of the magnetic field. These authors' results showed that when the two CMEs had magnetic fields with the same sense of rotation, they eventually merged, which could also be referred to as “CME-cannibalism”, as mentioned by Gopalswamy *et al.* (2001). When the two CMEs had an opposite field rotation, however, they interacted as in an elastic collision.

Based on a 3D MHD simulation, Lugaz *et al.* (2009) investigated the heliospheric evolution and the head-on interaction of two CMEs observed by SECCHI on 24–27 January 2007. The 3D simulation they used was the space weather modeling framework (SWMF) (Tóth *et al.*, 2005, 2007, 2012), as summarized in Lugaz *et al.* (2008). The solar wind and coronal magnetic field were simulated using the model developed by Cohen *et al.* (2007). This model used solar magnetogram data and the Wang–Sheeley–Arge (WSA) model (Wang, Sheeley, and Nash, 1990). To model the CMEs, Lugaz *et al.* (2009) used a semi-circular flux rope prescribed by a given total toroidal current, as done by Titov and Démoulin (1999). Lugaz *et al.* (2009) made a detailed comparison between the observations

and synthetic images from the numerical model, including time-elongation maps for several position angles. They found that their simulation could successfully reproduce the observations in LASCO FOV. It was also the first time that this type of event could be tracked with actual observations in the heliosphere. No deceleration of the two CMEs was assumed, and both CMEs were expected to merge around 21:00 UT on 25 January according to the time-height data from LASCO, but in the simulation, the merging occurred around 06:00 UT on 26 January, suggesting a strong interaction between the CMEs. Based on the 3D MHD simulation of the same CME–CME interaction event on 24–27 January 2007, Lugaz, Vourlidas, and Roussev (2009) compared two reconstruction techniques based on the point-P and FP approximations, which were used to derive the CME positions from elongation angle measurements. Then, the two techniques were applied to study the 1D head-on collision between the two CMEs.

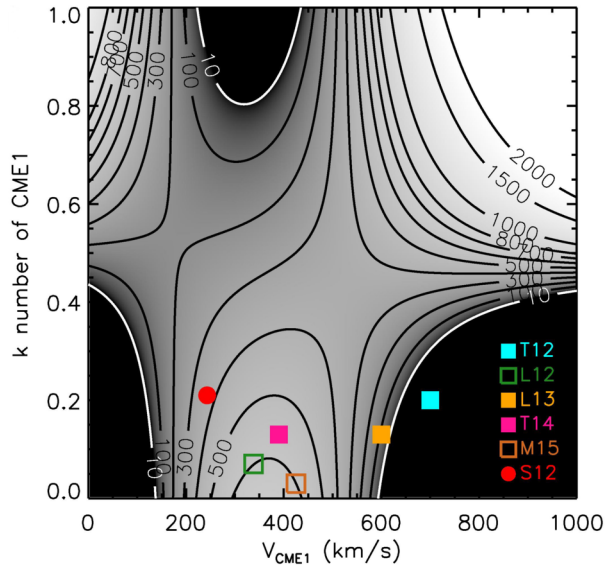
Furthermore, Lugaz *et al.* (2013) studied the influence on the head-on interaction of the relative orientation of the two CMEs by using 3D MHD numerical simulations. To determine the effect of the CME orientations on the resulting complex structure, they performed four different simulations (cases A, B, C, and D) with the axis of the second CME rotated by 90° from one simulation to the next. Each MHD simulation was performed in 3D with the SWMF in an idealized setting reminiscent of solar minimum conditions. The solar wind model used was the model of van der Holst *et al.* (2010), where Alfvén waves drove the solar wind. The simulations were performed with a single fluid (same electron and proton temperature) and no heat conduction. The CMEs were initiated with the flux rope model of Gibson and Low (1998), and the second CME was launched seven hours after the first from the same latitude and longitude at the solar surface.

Lugaz *et al.* (2013) showed that the center of the first CME was accelerated from about 600 km s^{-1} before the interaction to 750, 650, 800, and 62 km s^{-1} for cases A, B, C, and D, respectively, after the interaction. Meanwhile, the center of the second CME had a pre-interaction speed of 1500, 1000, 2000, and 1400 km s^{-1} and a post-interaction speed of 700, 650, 725, and 625 km s^{-1} , respectively. Determining the masses of the two CMEs was not straightforward; the authors assumed that the masses of the two CMEs were the same at the time of the interaction. If it were a perfectly inelastic collision, the second CME was expected to move with a speed of $V_{\text{inelast}} = 0.5 \times (V_{\text{CME1}} + V_{\text{CME2}})$, which was 1050, 800, 1300, and 1000 km s^{-1} , respectively, for the four cases. Therefore, this result was similar to that of Temmer *et al.* (2012) for the ejection of 1 August 2010, *i.e.* the collision was more likely to be superinelastic or a merging process.

Shen *et al.* (2013) applied a 3D MHD simulation to study the oblique collision process of two CMEs based on the observations of the November 2008 event and tried to understand the nature of the collision through the analysis of the energy transformation. Furthermore, Shen *et al.* (2016) carried out a series of 3D numerical experiments to study the dependence of the nature of the collision on the CME speed and k -number, the ratio of the CME kinetic energy to the CME total energy.

In the aforementioned studies, a 3D corona-interplanetary total variation diminishing (COIN-TVD) scheme was used (Shen *et al.*, 2011, 2012b). The background solar wind was constructed based on the observed line-of-sight magnetic field for Carrington rotation 2076 (Shen *et al.*, 2013, 2016). Two high-density, -velocity, and -temperature magnetized plasma blobs were superimposed successively on a background solar wind medium (Chané *et al.*, 2005; Shen *et al.*, 2011). Shen *et al.* (2013) considered the propagation directions of the initial plasma blobs to be N6W28 and N16W08, which were consistent with the directions of the two interacting CMEs of 2–8 November 2008. Shen *et al.* (2016) set the two initial directions of the CMEs as N11W18, which was between the directions of the two CMEs in Shen *et al.* (2013).

Figure 5 The surface of the critical approaching speed in the (V_{CME1}, k) space. Previously studied events are marked by *color-coded symbols*: the *dot* stands for superelastic and the *squares* for inelastic collisions. The *filled symbols* mean that the event is in agreement with the diagram derived from our numerical experiments, and the *open symbols* mean an almost disagreement (from Shen *et al.*, 2016). Licensed under a Creative Commons Attribution 4.0 International License.



Since CMEs may expand with a changing rate, Shen *et al.* (2013) used the energy definition to classify the collision types of the simulated events. Because the boundary of the CMEs could not be exactly identified as a result of some limitations of the MHD code (Shen *et al.*, 2013, 2016), instead of studying the energy changes of individual CMEs, the authors analyzed the variations of all types of energies integrated over the whole computational domain. In order to validate that the kinetic energy gain (or part of it) came from the collision, a reference case for each simulation was constructed for comparison, in which one of the two CMEs was introduced in an opposite direction to the other, so that the two CMEs were prevented from colliding.

Simulation results in Shen *et al.* (2013) showed that the kinetic energy gained in the case of collision was higher than that in the case of no collision, although the initial conditions of the two CMEs and the background solar wind were exactly the same. According to the energy definition, the total kinetic energy of the colliding system increased during the collision, the collision between the two CMEs was superelastic, through which additional magnetic and thermal energies were converted into kinetic energy (Shen *et al.*, 2013). As we described in Section 2, the energy definition used in Shen *et al.* (2013, 2016) was different from the classical Newtonian definition. The two definitions are equivalent only when the expansion speeds of the two colliding CMEs are almost unchanged during the collision. Thus, although Shen *et al.* (2013) simulated the CME collision event reported by Shen *et al.* (2012a) and their results showed that the total kinetic energy of the colliding system increased during the collision, they could not numerically prove that this could be a superelastic collision under Newton's definition.

Based on MHD simulations, Shen *et al.* (2016) demonstrated the dependence of the nature of the collision on the CME speed and k -number, as shown in Figure 5. The plot gives the fitting surface of the critical approaching speed in the (V_{CME1}, k) space. It was found that with a low approaching speed, the collision tends to be superelastic. It might be hard to achieve a superelastic collision in the three dark regions of the diagram, and the upper right corner seems to be the most favorable region to have a superelastic collision. This result was recently supported by the observational study of Mishra, Wang, and Srivastava (2016).

5. Summary and Discussion

In this review, we first presented four definitions of different types of collisions, which are a classical Newtonian definition, an energy definition, Poisson's definition, and Stronge's definition. In the presence of friction, these definitions are not always equivalent. The first two definitions are most widely used. In Newton's definition, the colliding objects do not expand, the centroid kinetic energy of the colliding objects could be used to determine the nature of the collision. When the objects considered are expanding or contracting with a changing rate, the energy definition is not equivalent to Newton's definition. Then, we reviewed some research works that were aimed at studying the nature of the collision of CMEs, *e.g.* inelastic collision, elastic collision, and the superelastic collision, by assuming a 1D head-on collision or analyzing an oblique collision in 3D. Particularly, we reviewed the existing numerical methods for simulating CME collisions. In most studies, the classical Newtonian definition was used to determine the nature of the collision, but in the simulations by Shen *et al.* (2013, 2016) the energy definition was used.

Previous results from the studies on the nature of CME–CME collisions are summarized in Table 1. It can be seen that almost all of the observational studies based on a 1D head-on collision model yielded an inelastic, perfectly inelastic, or merging-like collision, whereas some observational studies based on a 3D oblique collision model yielded a high possibility of a superelastic collision. Observational analysis and numerical simulations based on a 3D collision picture both suggested that a low approaching speed of two CMEs is favorable for a superelastic nature.

In most of the previous studies, the analysis of the nature of the collision was approximate. The collision process of CMEs is quite complex. The duration of a collision can exceed 10 hours, which is much longer than the normal collision process described in Newton's definition. The models used in both observational and numerical studies contain many ideal assumptions. Thus, the whole process of CME–CME collisions is still not clear enough. Up to now, none of the previous studies on collisions showed the separation of two colliding CMEs after a collision. Therefore the collision between CMEs cannot be considered as an ideal collision process in the context of a classical Newtonian definition. This issue might be attributed to the limitation of the observational technique and numerical methods, and is worth to be pursued in the future.

Different physical characteristics of the CME plasma may result in different types of collisions. The restitution coefficient estimated for the CMEs by the Newtonian definition seems to be a fairly reasonable approach, but we probably need to determine which definition is more suitable for the observed CMEs in a real scenario, as was also discussed in Mishra, Wang, and Srivastava (2016). Although the different definitions for the restitution coefficient are not always equivalent, there seems to be an agreement that the approaching speed of the two colliding objects may influence the restitution coefficient. When studying the restitution coefficient of a planar two-body collision both in the case of central collision (*e.g.* Chang and Ling, 1992) and eccentric collision (Adams and Tran, 1993), the restitution coefficients were found to decrease with increasing approaching velocity normal to the contact interface of the two colliding bodies, which is in strong agreement with the studies by Mishra, Wang, and Srivastava (2016) and Shen *et al.* (2016).

Although some simulations have been carried out to study the collision nature of CMEs, there are several pending issues. First of all, the CME-driven shock should be considered. As we discussed in Shen *et al.* (2016; see also Lugaz, Vourlidis, and Roussev, 2009), the CME-driven shock could change the dynamics of the CME that it is propagating, and may influence the nature of the two interacting CMEs significantly. However, how a shock changes the

Table 1 Summary of the previous studies on the nature of CME–CME collisions.

Method	Events	Collision nature	Ref.
1D	30 July – 1 August 2010	Inelastic	Liu <i>et al.</i> (2012)
	25 and 27 September 2012		Liu <i>et al.</i> (2014)
	14 – 15 February 2011		Maričić <i>et al.</i> (2014)
	14 – 15 February 2011		Shanmugaraju <i>et al.</i> (2014)
	23 – 24 May 2010	Likely perfectly inelastic	Lugaz <i>et al.</i> (2012)
	30 July – 1 August 2010	Merging-like process (superinelastic)	Temmer <i>et al.</i> (2012)
	14 – 15 February 2011		Temmer <i>et al.</i> (2014)
	Simulation case(s)		Lugaz <i>et al.</i> (2013)
	24 – 27 January 2007	Unknown	Lugaz, Vourlidas, and Roussev (2009)
1D, momentum conservation	14 – 15 February 2011	Inelastic	Mishra and Srivastava (2014)
	9 – 10 November 2012	Perfectly inelastic	Mishra, Srivastava, and Chakrabarty (2015)
	25 and 28 September 2012	Close to elastic	Mishra, Srivastava, and Singh (2015)
3D	5 March 2012	Likely to be superelastic	Colaninno and Vourlidas (2015)
3D, momentum conservation, propagation speed	2 – 8 November 2008	Superelastic with a likelihood of 73%	Shen <i>et al.</i> (2012a)
	25 October 2013	Most likely to be inelastic, high expansion speed, and low approaching speed increase the likelihood of the superelastic collision	Mishra, Wang, and Srivastava (2016)
2.5D MHD simulation	Simulation cases	Merging-like process (superinelastic) for the case of the same field rotation and similar to an elastic collision for the case of opposite field rotation	Schmidt and Cargill (2004)
3D MHD simulation	24 – 27 January 2007	Merging-like process	Lugaz <i>et al.</i> (2009)
3D MHD simulation, energy definition	2 – 8 November 2008	Super elastic	Shen <i>et al.</i> (2013)
	Simulation cases	Super elastic for a low approaching speed	Shen <i>et al.</i> (2016)

collision process is still unclear. In the studies by Shen *et al.* (2013, 2016), the shock was simply treated as a part of its associated CME and was not investigated separately. A detailed analysis of the role of the CME-driven shock is therefore needed using simulations. In addition, other influencing factors such as magnetic reconnection, the approaching angle,

the heliocentric distance of the collision, and the background solar wind were not fully explored in the numerical simulations by, *e.g.*, Shen *et al.* (2013, 2016). Furthermore, another major limitation of these numerical studies is that the authors cannot mark the boundaries of the CMEs during their propagation and interaction. In order to determine the nature of the collision, Shen *et al.* (2013, 2016) calculated the kinematic energy difference between a collision case and a non-collision case, which might be erroneous and may lead to inaccurate interpretations.

In general, there is a large scope for observational and numerical studies on the nature of CME–CME collisions toward understanding the sufficient conditions for inelastic or superelastic collisions, and to reveal the physical mechanism governing the collision process of CMEs.

Acknowledgements We acknowledge the constructive discussion with Chuanyi Tu from Peking University, who pointed out the difference between the classic Newtonian definition of a collision and the energy definition for colliding objects with a changing expanding speed, and the weaknesses and limitations in the analysis of the collision nature. F. Shen appreciates the discussion with Jiansen He from Peking University and Xin Wang from Beihang University. We are also grateful to the referee and the Guest Editor for improving the quality of the manuscript. F.S and X.F are supported by the grants from NSFC No. 41474152 and 41531073, Y.W and C.S are supported by the grants from NSFC No. 41574165, 41131065, 41274173, and 41421063. This work is also supported by the grants from the Specialized Research Fund for State Key Laboratories, and the National Program for Support of Top-notch Young Professionals. Some of the figures in this article have been published by permission of the AAS as indicated in the text.

Disclosure of Potential Conflicts of Interest The authors declare that they have no conflicts of interest.

Open Access This article is distributed under the terms of the Creative Commons Attribution 4.0 International License (<http://creativecommons.org/licenses/by/4.0/>), which permits unrestricted use, distribution, and reproduction in any medium, provided you give appropriate credit to the original author(s) and the source, provide a link to the Creative Commons license, and indicate if changes were made.

References

- Adams, G.G., Tran, D.N.: 1993, The coefficients of restitution of a planar 2-body eccentric impact. *ASME J. Appl. Mech.* **60**, 1058. DOI.
- Beer, F.P., Johnston, E.R. Jr., Clausen, W.E.: 2007, *Vector Mechanics for Engineers: Dynamics*. McGrawHill, New York.
- Brach, R.M.: 1984, Friction, restitution, and energy loss in planar collisions. *ASME J. Appl. Mech.* **51**, 164.
- Brogliato, B.: 1996, In: Thoma, M. (ed.) *Nonsmooth Impact Mechanics: Models, Dynamics and Control, Lecture Notes in Control and Inform. Sci.* **220**, Springer, New York.
- Burlaga, L.F., Behannon, K.W., Klein, L.W.: 1987, Compound streams, magnetic clouds, and major geomagnetic storms. *J. Geophys. Res.* **92**, 5725. DOI.
- Burlaga, L.F., Plunkett, S.P., St. Cyr, O.C.: 2002, Successive CMEs and complex ejecta. *J. Geophys. Res.* **107**(A10), 1266. DOI.
- Chané, E., Jacobs, C., Van der Holst, B., Poedts, S., Kimpe, D.: 2005, On the effect of the initial magnetic polarity and of the background wind on the evolution of CME shocks. *Astron. Astrophys.* **432**, 331. DOI.
- Chang, W.R., Ling, F.F.: 1992, Normal impact model of rough surfaces. *ASME J. Tribol.* **114**, 439. DOI.
- Cohen, O., Sokolov, I.V., Roussev, I.I., *et al.*: 2007, A semi-empirical magnetohydrodynamical model of the solar wind. *Astrophys. J. Lett.* **654**, L163. DOI.
- Colaninno, R.C., Vourlidas, A.: 2009, First determination of the true mass of coronal mass ejections: a novel approach to using the two STEREO viewpoints. *Astrophys. J.* **698**, 852. DOI.
- Colaninno, R.C., Vourlidas, A.: 2015, Using multiple-viewpoint observations to determine the interaction of three coronal mass ejections observed on 2012 March 5. *Astrophys. J.* **815**, 70. DOI.
- Davies, J.A., Harrison, R.A., Rouillard, A.P., Sheeley, N.R., Perry, C.H., Bewsher, D., *et al.*: 2009, A synoptic view of solar transient evolution in the inner heliosphere using the heliospheric imagers on STEREO. *Geophys. Res. Lett.* **36**, 210. DOI.

- Davies, J.A., Harrison, R.A., Perry, C.H., Möstl, C., Lugaz, N., Rollett, T., *et al.*: 2012, A self-similar expansion model for use in solar wind transient propagation studies. *Astrophys. J.* **750**, 23. DOI.
- Davies, J.A., Perry, C.H., Trines, R.M.G.M., Harrison, R.A., Lugaz, N., Möstl, C., *et al.*: 2013, Establishing a stereoscopic technique for determining the kinematic properties of solar wind transients based on a generalized self-similarly expanding circular geometry. *Astrophys. J.* **776**, 1. DOI.
- Farrugia, C., Berdichevsky, D.: 2004, Evolutionary signatures in complex ejecta and their driven shocks. *Ann. Geophys.* **22**, 3679. DOI.
- Feng, L., Inhester, B., Gan, W.: 2015, Radial flow pattern of a slow coronal mass ejection. *Astrophys. J.* **805**, 113. DOI.
- Feng, L., Wang, Y., Shen, F., Shen, C., Inhester, B., Lu, L., Gan, W.: 2015, Why does the apparent mass of a coronal mass ejection increase? *Astrophys. J.* **812**, 70. DOI.
- Gibson, S., Low, B.C.: 1998, A time-dependent three-dimensional magnetohydrodynamic model of the coronal mass ejection. *Astrophys. J.* **493**, 1. DOI.
- Gopalswamy, N., Yashiro, S., Kaiser, M.L., Howard, R.A., Bougeret, J.-L.: 2001, Radio signatures of coronal mass ejection interaction: coronal mass ejection cannibalism? *Astrophys. J. Lett.* **548**, L91. DOI.
- Gopalswamy, N., Mäkelä, P., Xie, H., Akiyama, S., Yashiro, S.: 2009, CME interactions with coronal holes and their interplanetary consequences. *J. Geophys. Res.* **114**(A3), A00A22. DOI.
- Hayashi, K., Zhao, X.-P., Liu, Y.: 2006, MHD simulation of two successive interplanetary disturbances driven by cone-model parameters in IPS-based solar wind. *Geophys. Res. Lett.* **33**(20), L20103. DOI.
- Howard, T.A., Tappin, S.J.: 2008, Three-dimensional reconstruction of two solar coronal mass ejections using the STEREO spacecraft. *Solar Phys.* **252**, 373. DOI.
- Howard, T.A., Fry, C.D., Johnston, J.C., Webb, D.F.: 2007, On the evolution of coronal mass ejections in the interplanetary medium. *Astrophys. J.* **667**, 610. DOI.
- Inhester, B.: 2006, Stereoscopic basics for the STEREO mission. [arXiv](https://arxiv.org/abs/2006.03281).
- Jackson, J.D.: 1997, *Classical Electrodynamics*. Wiley, New York.
- Kahler, S.W., Webb, D.F.: 2007, V arc interplanetary coronal mass ejections observed with the Solar Mass Ejection Imager. *J. Geophys. Res.* **112**(A11), 9103. DOI.
- Kaiser, M.L., Kucera, T.A., Davila, J.M., St. Cyr, O.C., Guhathakurta, M., Christian, E.: 2008, The STEREO mission: an introduction. *Space Sci. Rev.* **136**, 5. DOI.
- Keller, J.B.: 1986, Impact with friction. *ASME J. Appl. Mech.* **53**, 1.
- König, J.: 1905, Zum Kontinuum-problem. *Math. Ann.* **60**(2), 177. DOI.
- Liu, Y., Davies, J.A., Luhmann, J.G., Vourlidas, A., Bale, S.D., Lin, R.P.: 2010, Geometric triangulation of imaging observations to track coronal mass ejections continuously out to 1 AU. *Astrophys. J. Lett.* **710**, L82. DOI.
- Liu, Y.D., Luhmann, J.G., Möstl, C., Martinez-Oliveros, J.C., Bale, S.D., Lin, R.P., *et al.*: 2012, Interactions between coronal mass ejections viewed in coordinated imaging and in situ observations. *Astrophys. J. Lett.* **746**, 2. DOI.
- Liu, Y.D., Yang, Z., Wang, R., Luhmann, J.G., Richardson, J.D., Lugaz, N.: 2014, Sun-to-Earth characteristics of two coronal mass ejections interacting near 1 AU: formation of a complex ejecta and generation of a two-step geomagnetic storm. *Astrophys. J. Lett.* **793**, L41. DOI.
- Louge, M.Y., Adams, M.E.: 2002, Anomalous behavior of normal kinematic restitution in the oblique impacts of a hard sphere on an elastoplastic plate. *Phys. Rev. E* **65**, 021303. DOI.
- Lubarda, V.A.: 2010, The bounds on the coefficients of restitution for the frictional impact of rigid pendulum against a fixed surface. *ASME J. Appl. Mech.* **77**, 011006. DOI.
- Lugaz, N., Manchester, I.W.B., Gombosi, T.I.: 2005, Numerical simulation of the interaction of two coronal mass ejections from Sun to Earth. *Astrophys. J.* **634**(1), 651. DOI.
- Lugaz, N., Rousev, I.I.: 2011, Numerical modeling of interplanetary coronal mass ejections and comparison with heliospheric images. *J. Atmos. Solar-Terr. Phys.* **73**(10), 1187. DOI.
- Lugaz, N., Vourlidas, A., Rousev, I.I.: 2009, Deriving the radial distances of wide coronal mass ejections from elongation measurements in the heliosphere application to CME–CME interaction. *Ann. Geophys.* **27**(9), 3479. DOI.
- Lugaz, N., Vourlidas, A., Rousev, I.I., Jacobs, C., Manchester, W.B. IV, Cohen, O.: 2008, The brightness of density structures at large solar elongation angles: what is being observed by STEREO SECCHI? *Astrophys. J. Lett.* **684**, 111. DOI.
- Lugaz, N., Vourlidas, A., Rousev, I.I., Morgan, H.: 2009, Solar-terrestrial simulation in the STEREO era: the January 24–25, 2007 eruptions. *Solar Phys.* **256**, 269. DOI.
- Lugaz, N., Hernandez-Charpak, J.N., Rousev, I.I., Davis, C.J., Vourlidas, A., Davies, J.A.: 2010, Determining the azimuthal properties of coronal mass ejections from multi-spacecraft remote-sensing observations with STEREO SECCHI. *Astrophys. J.* **715**, 493. DOI.
- Lugaz, N., Farrugia, C.J., Davies, J.A., Möstl, C., Davis, C.J., Rousev, I.I., Temmer, M.: 2012, The deflection of the two interacting coronal mass ejections of 2010 May 23–24 as revealed by combined in situ measurements and heliospheric imaging. *Astrophys. J.* **759**, 68. DOI.

- Lugaz, N., Farrugia, C.J., Manchester, W.B., Schwadron, N.: 2013, The interaction of two coronal mass ejections: influence of relative orientation. *Astrophys. J.* **778**, 20. DOI.
- Lugaz, N., Temmer, M., Wang, Y., Farrugia, C.: 2017, The interaction of successive coronal mass ejections: a review. *Solar Phys.* **292**, 64. DOI.
- MacQueen, R.M., Eddy, J.A., Gosling, J.T., Hildner, E., Munro, R.H., Newkirk, G.A. Jr., Poland, A.I., Ross, C.L.: 1974, The outer solar corona as observed from Skylab: preliminary results. *Astrophys. J.* **187**, L85. DOI.
- Maričić, D., Vršnak, B., Dumbović, M., Žic, T., Roša, D., Hržina, D., et al.: 2014, Kinematics of interacting ICMEs and related Forbush decrease: case study. *Solar Phys.* **289**, 351. DOI.
- Martínez-Oliveros, J.C., Raftery, C.L., Bain, H.M., Liu, Y., Krupar, V., Bale, S., Krucker, S.: 2012, The 2010 August 1 type II burst: a CME–CME interaction and its radio and white-light manifestations. *Astrophys. J.* **748**, 66. DOI.
- Mishra, W., Srivastava, N.: 2014, Morphological and kinematic evolution of three interacting coronal mass ejections of 2011 February 13–15. *Astrophys. J.* **794**, 64. DOI.
- Mishra, W., Srivastava, N., Chakrabarty, D.: 2015, Evolution and consequences of interacting CMEs of 9–10 November 2012 using STEREO/SECCHI and in situ observations. *Solar Phys.* **290**, 527. DOI.
- Mishra, W., Srivastava, N., Singh, T.: 2015, Kinematics of interacting CMEs of 25 and 28 September 2012. *J. Geophys. Res.* **120**, 10. DOI.
- Mishra, W., Wang, Y., Srivastava, N.: 2016, On understanding the nature of collision of coronal mass ejections observed by STEREO. *Astrophys. J.* **831**, 99. DOI.
- Saitoh, K., Bodrova, A., Hayakawa, H., Brilliantov, N.V.: 2010, Negative normal restitution coefficient found in simulation of nanocluster collisions. *Phys. Rev. Lett.* **105**, 238001. DOI.
- Schmidt, J., Cargill, P.: 2004, A numerical study of two interacting coronal mass ejections. *Ann. Geophys.* **22**, 2245. DOI.
- Schwenn, R., dal Lago, A., Huttunen, E., Gonzalez, W.D.: 2005, The association of coronal mass ejections with their effects near the Earth. *Ann. Geophys.* **23**, 1033. DOI.
- Shanmugaraju, A., Prasanna Subramanian, S., Vrsnak, B., Ibrahim, M.S.: 2014, Interaction between two CMEs during 14–15 February 2011 and their unusual radio signature. *Solar Phys.* **289**, 4621. DOI.
- Shen, F., Feng, X.S., Wang, Y., Wu, S.T., Song, W.B., Guo, J.P., Zhou, Y.F.: 2011, Three-dimensional MHD simulation of two coronal mass ejections' propagation and interaction using a successive magnetized plasma blobs model. *J. Geophys. Res.* **116**(A09), 103. DOI.
- Shen, C., Wang, Y., Wang, S., Liu, Y., Liu, R., Vourlidis, A., et al.: 2012a, Super-elastic collision of large-scale magnetized plasmoids in the heliosphere. *Nat. Phys.* **8**, 923. DOI.
- Shen, F., Wu, S.T., Feng, X., Wu, C.-C.: 2012b, Acceleration and deceleration of coronal mass ejections during propagation and interaction. *J. Geophys. Res.* **117**(A11), 101. DOI.
- Shen, F., Shen, C., Wang, Y., Feng, X., Xiang, C.: 2013, Could the collision of CMEs in the heliosphere be super-elastic? Validation through three-dimensional simulations. *Geophys. Res. Lett.* **40**, 1457. DOI.
- Shen, F., Wang, Y., Shen, C., Feng, X.: 2016, Turn on the super-elastic collision nature of coronal mass ejections through low approaching speed. *Sci. Rep.* **6**, 19576. DOI.
- Stewart, D.E.: 2000, Rigid-body dynamics with friction and impact. *SIAM Rev.* **42**, 3. DOI.
- Stronge, W.J.: 1990, Rigid body collisions with friction. *Proc. Roy. Soc. London Ser. A* **431**, 169. DOI.
- Temmer, M., Vršnak, B., Rollett, T., Bein, B., de Koning, C.A., Liu, Y.D., et al.: 2012, Characteristics of kinematics of a coronal mass ejection during the 2010 August 1 CME–CME interaction event. *Astrophys. J.* **749**, 57. DOI.
- Temmer, M., Veronig, A.M., Peinhart, V., Vršnak, B.: 2014, Asymmetry in the CME–CME interaction process for the events from 2011 February 14–15. *Astrophys. J.* **785**, 85. DOI.
- Thernisien, A.F.R.: 2011, Implementation of the graduated cylindrical shell model for the three-dimensional reconstruction of coronal mass ejections. *Astrophys. J. Suppl.* **194**, 33. DOI.
- Thernisien, A.F.R., Howard, R.A., Vourlidis, A.: 2006, Modeling of flux rope coronal mass ejections. *Astrophys. J.* **652**, 1. DOI.
- Thernisien, A.F.R., Vourlidis, A., Howard, R.A.: 2009, Forward modeling of coronal mass ejections using STEREO/SECCHI data. *Solar Phys.* **256**, 111. DOI.
- Thompson, W.T.: 2009, 3D triangulation of a Sun-grazing comet. *Icarus* **200**, 351. DOI.
- Titov, V.S., Démoulin, P.: 1999, Basic topology of twisted magnetic configurations in solar flares. *Astron. Astrophys.* **351**, 707.
- Tóth, G., Sokolov, I.V., Gombosi, T.I., Chesney, D.R., Clauer, C.R., de Zeeuw, D.L., et al.: 2005, Space Weather Modeling Framework: a new tool for the space science community. *J. Geophys. Res.* **110**, A12226. DOI.
- Tóth, G., De Zeeuw, D.L., Gombosi, T.I., Manchester, W.B., Ridley, A.J., Sokolov, I.V., Roussev, I.I.: 2007, Sun-to-thermosphere simulation of the 28–30 October 2003 storm with the Space Weather Modeling Framework. *Space Weather* **5**, S06003. DOI.

- Tóth, G., van der Holst, B., Sokolov, I.V., De Zeeuw, D.L., Gombosi, T.I., Fang, F., *et al.*: 2012, Adaptive numerical algorithms in space weather modelling. *J. Comput. Phys.* **231**, 870. DOI.
- Tousey, R., Bartoe, J.D.F., Bohlin, J.D., Brueckner, G.E., Purcell, J.D., Scherrer, V.E., *et al.*: 1973, A preliminary study of the extreme ultraviolet spectroheliograms from Skylab. *Solar Phys.* **33**, 265. DOI.
- van der Holst, B., Manchester, W.B., Frazin, R.A., Vásquez, A.M., Tóth, G., Gombosi, T.I.: 2010, A data-driven, two-temperature solar wind model with Alfvén waves. *Astrophys. J.* **725**, 1373. DOI.
- Vourlidas, A., Howard, R.A.: 2006, The proper treatment of coronal mass ejection brightness: a new methodology and implications for observations. *Astrophys. J.* **642**, 1216. DOI.
- Vourlidas, A., Subramanian, P., Dere, K.P., Howard, R.A.: 2000, Large-angle spectrometric coronagraph measurements of the energetics of coronal mass ejections. *Astrophys. J.* **534**, 456. DOI.
- Wang, Y., Mason, M.T.: 1992, Two-dimensional rigid body collisions with friction. *ASME J. Appl. Mech.* **59**, 635. DOI.
- Wang, Y.M., Sheeley, N.R., Nash, A.G.: 1990, Latitudinal distribution of solar-wind speed from magnetic observations of the sun. *Nature* **347**, 439. DOI.
- Wang, Y.M., Wang, S., Ye, P.Z.: 2002, Multiple magnetic clouds in interplanetary space. *Solar Phys.* **211**, 333. DOI.
- Wang, Y.M., Ye, P.Z., Wang, S.: 2003, Multiple magnetic clouds: several examples during March–April. *J. Geophys. Res.* **108**, 1370. DOI.
- Wang, Y., Chen, C., Gui, B., Shen, C., Ye, P., Wang, S.: 2011, Statistical study of coronal mass ejection source locations: understanding CMEs viewed in coronagraphs. *J. Geophys. Res.* **116**, A04104. DOI.
- Webb, D.F., Howard, T.A., Fry, C.D., *et al.*: 2009, Study of CME propagation in the inner heliosphere: SOHO LASCO, SMEI and STEREO HI observations of the January 2007 events. *Solar Phys.* **256**, 239. DOI. 2007.
- Webb, D.F., Möstl, C., Jackson, B.V., Bisi, M.M., Howard, T.A., Mulligan, T., *et al.*: 2013, Heliospheric imaging of 3D density structures during the multiple coronal mass ejections of late July to early August 2010. *Solar Phys.* **285**, 317. DOI.
- Wood, B.E., Howard, R.A., Plunkett, S.P., Socker, D.G.: 2009, Comprehensive observations of a solar minimum coronal mass ejection with the solar terrestrial relations observatory. *Astrophys. J.* **694**, 707. DOI.
- Wu, S.T., Wang, A.H., Gopalswamy, N.: 2002, MHD modeling of CME and CME interactions in a bi-model solar wind: a preliminary analysis of the 20 January 2001 two CMEs interaction event. In: *ESA SP-505: SOLMAG 2002. Proceedings of the Magnetic Coupling of the Solar Atmosphere Euroconference*, 227.
- Xiong, M., Zheng, H., Wang, S.: 2009, Magnetohydrodynamic simulation of the interaction between two interplanetary magnetic clouds and its consequent geoeffectiveness: 2. Oblique collision. *J. Geophys. Res.* **114**, A11101. DOI.
- Xiong, M., Zheng, H., Wu, S.T., Wang, Y., Wang, S.: 2007, Magnetohydrodynamic simulation of the interaction between two interplanetary magnetic clouds and its consequent geoeffectiveness. *J. Geophys. Res.* **112**, A11103. DOI.
- Yao, W., Chen, B., Liu, C.: 2005, Energetic coefficient of restitution for planar impact in multi-rigid-body systems with friction. *Int. J. Impact Eng.* **31**, 255. DOI.